photonics

MDPI

Review

Broadband Terahertz Metal-Wire Signal Processors: A Review

Mohammad Ghazialsharif, Junliang Dong *, Alaeddine Abbes and Roberto Morandotti *

Centre Énergie Matériaux Télécommunications, Institut National de la Recherche Scientifique, Varennes, QC J3X 1P7, Canada

* Correspondence: Junliang.Dong@inrs.ca (J.D.); Roberto.Morandotti@inrs.ca (R.M.)

Abstract: Communication links operating at terahertz frequencies are envisioned to provide a revolutionary enhancement of data transmission. As fundamental building blocks, waveguides play an indispensable role in future terahertz networks, not only transporting data streams with unprecedented data rates, but also serving as a versatile platform for signal processing. Among various terahertz waveguides, metal-wire waveguides have attracted particular attention due to their distinct characteristics, such as structural simplicity, broad operating bandwidths, low transmission losses, and low dispersion, in turn making them promising candidates for signal processing. However, because of the tight confinement of modal energy within the wavelength-scale space, manipulating the propagating terahertz signals in-between the metal-wires is challenging. Here, we report the most recent advances in the realization of signal-processing functionalities within metal-wire waveguides. Based on these state-of-the-art methodologies, broadband signal processors that can function as filters, couplers, temporal integrators, as well as multiplexers, have been obtained. We expect this review to inspire new terahertz metal-wire signal processors with high potential for real-time tunability and reconfigurability.

Keywords: terahertz; metal-wire waveguides; signal processing; terahertz communications

Citation: Ghazialsharif, M.; Dong, J.; Abbes, A.; Morandotti, R. Broadband Terahertz Metal-Wire Signal Processors: A Review. *Photonics* **2023**, *10*, 48. https://doi.org/10.3390/photonics10010048

Received: 21 August 2022
Revised: 23 December 2022
Accepted: 27 December 2022
Published: 3 January 2023

1. Introduction

Carrying data-streams using terahertz (THz) radiation (with frequencies spanning the range between 0.1 THz and 10 THz) represents the ultimate technology for the next six-generation (6G) communication networks [1–3]. Indeed, with respect to millimeter waves used in the 5G networks, the THz spectral region offers higher available bandwidth and could meet the ever-growing demand for higher data-rates, aiming at terabits-per second (Tb/s) [4]. In order to accommodate the capacity for such unprecedented data-rates, it is necessary to develop a new series of components [5], such as modulators, switches, couplers, filters, and multiplexers, that can serve as the fundamental blocks for manipulating THz communication signals.

Over the last decades, a substantial amount of effort has been dedicated to the design of low-loss and low-dispersion THz waveguides, in order to transport THz signals efficiently from one point to another. In general, THz waveguides can be divided into two major categories: dielectric and metallic waveguides. THz dielectric waveguides [6] are considered promising candidates due to the feasibility of refractive index engineering and straightforward manufacturing techniques, such as 3D printing [7–9]. However, the THz propagation modes within dielectric waveguides suffer from significant frequency-dependent absorption losses and dispersion [10,11]. To overcome these issues, low-loss polymers [8], such as Zeonex and TOPAS (cyclic olefin copolymer), have been identified, and various waveguide structures have been explored, including porous polymer fibers [12], periodically microstructured fibers [13], bandgap fibers [14], as well as fibers with rectangular slot air-holes [15]. Although dispersion can be tailored by means of a judicious design of waveguide structures so that a low-dispersion response can be achieved at certain THz frequencies, it is extremely difficult to design dielectric waveguides that can offer almost

zero dispersion for a broad THz frequency range. As a result, the operating bandwidths of THz dielectric waveguides are typically narrow [16], in turn making it impossible to manipulate broadband THz signals. THz metallic waveguides that are typically scaled-down versions of well-known guiding structures at radio and microwave frequencies, such as hollow rectangular [17] and coaxial [18] waveguides, experience strong dispersion near the cut-off frequency of the guiding mode. In contrast, THz metallic waveguides that can support transverse electromagnetic (TEM) modes, such as parallel-plate waveguides (PPWGs) [19] and two-wire waveguides (TWWGs) [20], are attractive alternatives due to their capabilities to support the low-loss and low-dispersion propagation of broadband THz pulses. In addition, hybrid THz waveguides, which incorporate dielectric cladding into metallic waveguides [21] or embed metal-wires into dielectric hollow-core fibers [22], have been demonstrated to further improve the performance of signal transporting. While the development of THz waveguides is not the main purpose of our review, we recognize that the design of compact and robust THz waveguides is an important research topic, which has been comprehensively reviewed in [6,8,16,17,21].

Besides signal transporting, another important function of THz waveguides is to serve as the seeding platform to realize broadband THz signal processing [23]. Recent progress has witnessed a dramatic boost in the development of signal-processing components based on PPWGs, such as power splitters [24], add-drop filters [25], as well as multiplexers/demultiplexers [26]. Compared to the large footprints of PPWGs, metal-wire waveguides feature several distinct advantages, such as structural simplicity, tolerance to bending [27], and affinity to cables for efficient and straightforward connections [28]. However, the realization of signal-processing functionalities based on THz metal-wire waveguides remains challenging. The underlying reason is that the modal energy is tightly confined in the wavelength-scale space between the metal-wires, which limits the possible ways to manipulate the propagating THz waves. In this review, we provide a comprehensive survey of the cutting-edge techniques which have been established in broadband THz signal processing, based on metal-wire waveguides. Section 2 provides a brief introduction to the signal guiding properties of THz metal-wire waveguides. Section 3 reports on three different methodologies for realizing signal-processing functionalities within metal-wire waveguides, including inserting standalone components, varying waveguide topologies/geometries, and engineering metal-wire surfaces. Finally, we discuss possible future advances in the field.

2. THz Guiding Properties of Metal-Wire Waveguides

In the THz frequency regime, metals are generally considered as perfect conductors, since the negligible penetration of the electromagnetic field leads to highly delocalized surface plasmon polaritons (SPPs) akin to grazing-incidence light fields. A single bare metal-wire, as shown in Figure 1a, can carry THz pulses with virtually no dispersion and low attenuation [29]. Single metal-wire waveguides (SWWGs), also known as 'Sommerfeld wires', support a transverse magnetic (TM) mode [30], i.e., TM_{01}, as shown in Figure 1b. Even though these waveguides support the propagation of high-order modes, such modes exhibit an attenuation coefficient so large that the SWWG quickly tends to become single mode after a short propagation distance. The first demonstration of a SWWG [29], consisting of a stainless steel wire with a diameter of 0.9 mm, featured an attenuation constant of less than 0.03 dB/cm, and almost no dispersion between 0.25 THz and 0.75 THz. However, SWWGs also show some significant drawbacks. First, their performance is extremely sensitive to perturbations [31], such as bending, leading to a loose confinement of the fundamental mode around the wire [32]. Another drawback is the low coupling efficiency [33]. Since the fundamental mode of SWWGs is radially polarized, commonly used sources emitting linearly polarized THz beams, such as photoconductive antennas, cannot be utilized for the efficient excitation of this mode.

On the contrary, two-wire waveguides (TWWGs), which consist of two metal-wires with an air gap between them (see Figure 1c), can be directly excited with a simple THz

dipole source, when its polarization is parallel to the line connecting the wire centers [21]. This is because the field distribution of its fundamental transverse electromagnetic (TEM) mode resembles that of a dipole, as shown in Figure 1d. In particular, the efficient confinement of the modal energy in-between the two wires, in contrast to the weakly guided Sommerfeld wave of a single wire, makes TWWGs more tolerant to bending losses [27]. A rigorous theoretical analysis of the two-wire waveguide can be found in [20]. To date, the typical material choice for TWWGs is copper, because of its excellent conductivity and good malleability. As reported in [34], a 1.1 dB/cm loss was experimentally achieved from 0.5 THz to 1.6 THz. A comparison between the behavior of copper and other commonly used metals at THz frequencies, such as gold, aluminum, stainless steel, and silver, is summarized in Table 1 [35]. Although silver shows better properties than copper, silver wires are less commercially available and are more expensive. In addition, TWWGs may suffer from electromagnetic interference due to their open environment configurations. In practice, dielectric claddings, such as polystyrene foam [21] and porous micro-structured polyethylene [36], can be implemented onto the TWWGs, in order to improve their mechanical stability and insensitivity to environmental variables.

Table 1. Properties of most used metals in terms of conductivity (σ_0) and skin depth (δ) at 1 THz.

	Cu	Ag	Au	Al	Stainless Steel [1]
$\sigma_0 (10^6 S \cdot m^{-1})$	59.6	63.0	45.2	37.8	1.45
$\delta (nm)$	65.2	63.4	74.9	81.9	418

[1]-Steel 304.

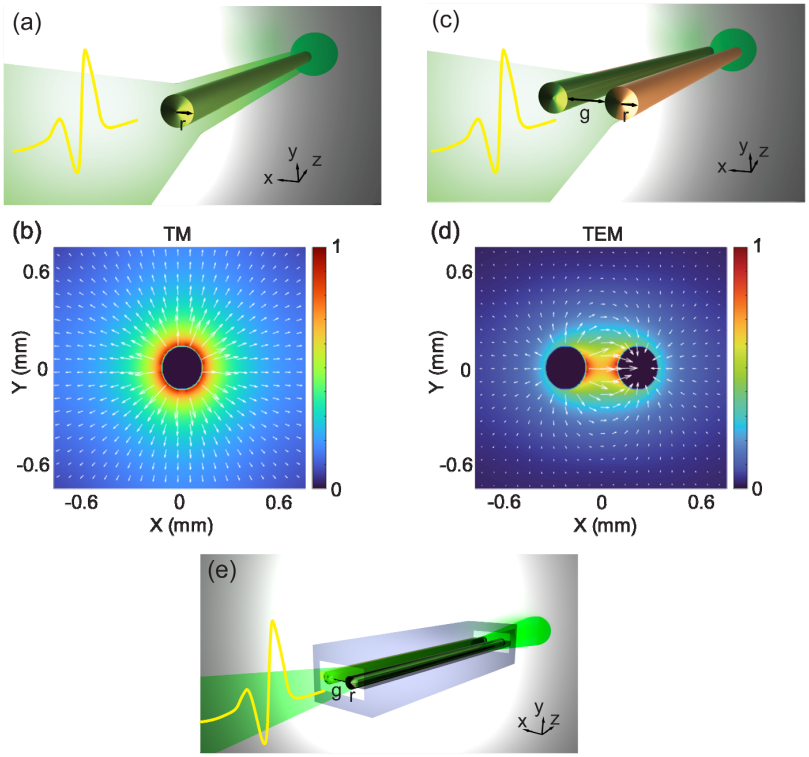

Figure 1. Schematics of typical THz metal−wire waveguides and their fundamental modes. (**a**) Schematic of the SWWG with a wire radius r = 127 µm. (**b**) Simulated electric field distributions of the fundamental TM mode at 0.5 THz. (**c**) Schematics of the TWWG waveguide with a wire radius r = 127 µm and an air gap g = 300 µm. (**d**) Simulated electric field distributions of the fundamental TEM mode at 0.5 THz. (**e**) The TWWG (wire radius r = 330 µm and the air gap g = 660 µm) fabricated via 3D printing and metal deposition, adapted from [37]. Arrows indicate the directions of local field polarization distributions.

Recently, 3D additive manufacturing has emerged as a promising technique for fabricating THz waveguides, due to the ubiquitous availability of hardware, the low threshold for production, as well as the ease of integration. In 2020, Cao et al., fabricated a TWWG using the combination of stereolithography (SLA) 3D printing and wet chemistry metal deposition [37]. Such a micro-encapsulated TWWG, as shown in Figure 1e, consisted of two complementary parts, each comprising one wire attached to a half cage using subwavelength dielectric support ridges. These parts were printed along the propagation direction, then the silver layer was deposited on top of the plastic wire using wet chemistry to form conductive surfaces with thicknesses of several microns. A two-wire waveguide was finally achieved where the two metallized parts were assembled into each other. By using the 3D additive manufacturing technique, reliable and compact TWWG components can be directly printed, which avoids the requirement of mounting straight metallic wires in bulky holders, in turn making it amenable to the realization of integrated platforms.

3. Broadband THz Metal-Wire Signal Processors

Here, we classify the state-of-the-art methods for the realization of various signal-processing functionalities within THz metal-wire waveguides into three categories: inserting standalone components into the waveguide, varying the topologies or geometries of the waveguide, and directly engineering the wire surfaces.

3.1. Inserting Standalone Components

Implanting dielectric materials into the air gap within the metal-wire waveguides is one of the first ideas that have been investigated. Because of the tight energy confinement between the two wires, the effective refractive index of the waveguide can be tuned by implanting a thin layer of dielectric materials into the air gap. For example, by inserting a micromachined paper grating into a TWWG, Yan et al. demonstrated a low-loss THz waveguide Bragg grating [38], as shown in Figure 2a. The paper grating was achieved by precision laser cutting of slit arrays in a regular 100-µm-thick printing paper with a refractive index of ~1.45. In this work, two waveguide Bragg gratings were fabricated, which featured Bragg resonances at 0.637 THz and 0.369 THz with Q-factors of 142 and 105, respectively.

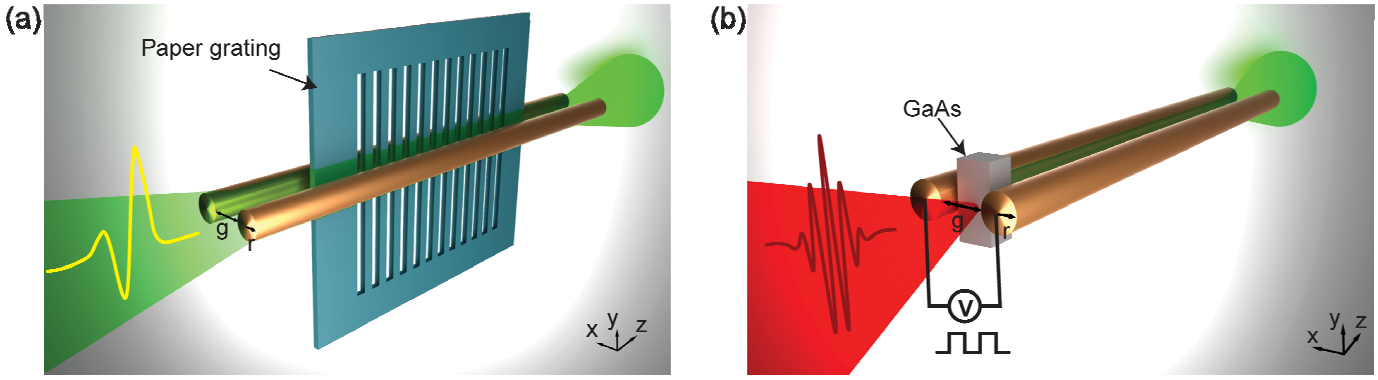

Figure 2. THz metal-wire signal processors realized by inserting standalone components. (**a**) Schematic of a THz waveguide Bragg grating (adapted from [38]), which was fabricated by using a TWWG with a wire radius r = 125 µm, an air gap g = 900 µm, and a paper grating with a thickness of 100 µm. The paper cut consisted of 90 slits (cut through) that were ~110 µm wide, with periods of ~226 µm and a total grating length of 2.1 cm. (**b**) Schematic of an active TWWG (adapted from [34]). A thin GaAs piece (300 µm × 300 µm × 5 mm) is inserted between the wires and serves as a semi-large area photoconductive antenna inside the TWWG (wire radius r = 250 µm and air gap g = 300 µm).

Similarly, by inserting a small piece of GaAs in-between the two wires, Mridha et al. demonstrated an active TWWG [34], in which the generation of THz signals occurred directly inside the guiding structure. Such a device can achieve efficient coupling of the THz radiation in a dispersion-less waveguide, in turn leading to a 60 times higher energy output under the same optical pump power and applied voltage. The excitation methodology is similar to that used in photoconductive antennas. This method brings new possibilities of THz signal processing. For example, by manipulating the optical pump power or the applied voltage, the amplitude of the generated THz signals can be modulated, in turn leading to the realization of a waveguide-integrated all-optical or electro-optical modulator for high-speed communication systems.

3.2. Varying Waveguide Geometries/Topologies

By exploiting the 3D additive manufacturing technique introduced in the previous section, TWWG components with complex shapes can be easily fabricated. In [37], Cao et al. demonstrated a Y-shaped coupler based on two fused TWWG bends with a 4 cm bending radius, as shown in Figure 3a. In addition, the wires of two TWWGs can be assembled adjacently to form an inter-waveguide directional coupler [39], as shown in Figure 3b. The propagating THz energy will couple from the through path to the other attached waveguide. The coupling length is frequency-dependent, being ~24.5 mm at ~0.14 THz. These couplers can be further used for the design of add-drops, multiplexers, and demultiplexers by incorporating additional filters into the splitter's ports. For example, by inserting a metallized paper grating into this Y-shaped THz power splitter, a three-port add-drop multiplexer can be achieved [37].

In the TWWGs, the propagating THz electric field is predominantly confined within the air gap between two wires. When the size of the air gap is adjusted to a subwavelength scale, the resultant field enhancement can also be exploited to realize signal processing. In 2021, Balistreri et al. demonstrated a broadband time-domain integrator based on a tapered TWWG [40]. Such a structure consists of two metal-wires separated by a varying air gap that narrows down to a subwavelength scale from the waveguide input to its output (gap size from 1100 μm down to 24 μm), as shown in Figure 3c. The tight confinement of THz energy in a subwavelength gap volume results in an enhanced THz electric field that is inversely proportional to the frequency, in turn leading to the time-domain integration of the THz signals. In particular, this time-domain integrator features an ultra-broadband operating bandwidth, potentially up to ~10 THz.

Furthermore, inspired by the TWWGs, Dong et al. recently introduced a new metal-wire waveguide topology, namely the four-wire waveguide (FWWG) [41]. Such a waveguide consists of four identical bare copper wires with an identical separation gap in free-space, as shown in Figure 3d. Due to the symmetrical arrangement of the four wires, the two fundamental modes, TEM_x (Figure 3e) and TEM_y (Figure 3f), exhibit symmetrical field profiles, which are equally divided into two identical portions along the axes. In particular, each portion of the field distribution is mainly confined in-between the two wires and shows a similar profile to that of the TWWG, thus indicating that the FWWG can also be efficiently excited by a linearly polarized THz input beam. In details, depending on the polarization states of the modes, TEM_x is excited by an x-polarized beam, while TEM_y is excited by a y-polarized beam. Most importantly, since the two fundamental modes are independent, two broadband THz signals with orthogonal polarization states can be transmitted without any interference. Consequently, the FWWG can be operated as a broadband polarization-division multiplexer. Due to its inherent broadband nature, the FWWG features significant potential in simultaneously supporting both frequency- and polarization-division multiplexing.

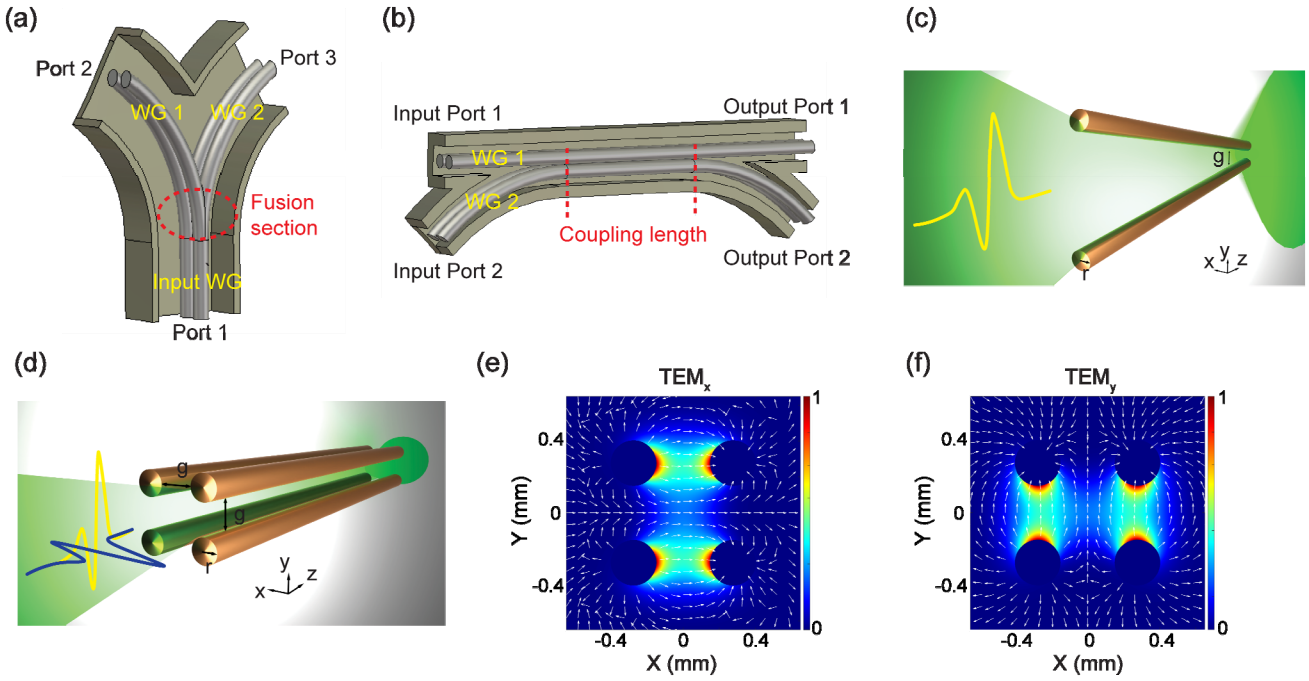

Figure 3. THz metal−wire signal processors realized by varying the geometries or topologies of the wires. (**a**) Schematic of a THz Y-shaped splitter that uses two fused TWWGs redirected into different paths, adapted from [37]. (**b**) Schematic of a THz directional coupler achieved by attaching two TWWGs, adapted from [39]. (**c**) Schematic of a THz time-domain integrator based on a tapered TWWG, adapted from [40]. The waveguide has an input gap of 1100 μm with a tapering angle of 0.36° and a total length of 85 mm. (**d**) Schematic of a THz polarization-division multiplexer based on a four-wire waveguide (FWWG), adapted from [41]. The FWWG is composed of four identical copper wires (r = 127 μm) placed in a square geometry, separated by an equal air gap (g = 300 μm). (**e**,**f**) Simulated electric field distributions of the fundamental TEM modes evaluated at 0.5 THz, TEM_x and TEM_y, which can be efficiently excited by x-polarized and y-polarized THz beams, respectively. The arrows in the 2D distributions indicate the local electric field polarization directions.

3.3. Engineering the Metal-Wire Surfaces

The propagation of THz SPPs along the metal-air interface is extremely sensitive to the metal surface condition. When periodic structures are engraved on the metal, surface waves resembling the behavior of SPPs, so-called spoof SPPs [42], can be still sustained. By varying the geometry of the periodic structures, the propagation characteristics of the spoof SPPs can be tailored accordingly. Therefore, engineering the metal-wire surfaces is able to provide a universal approach for manipulating the propagating THz waves within the waveguide. Depending on the size of the period, a subwavelength-scale periodic structure can be treated as an effective medium, while a wavelength-scale periodic structure behaves as a Bragg grating [43]. Figure 4a illustrates typical subwavelength-scale periodic grooves with width w = 35 μm, depth d = 40 μm, and period p = 80 μm, respectively. The dispersion relation is not linear and the group velocity of the spoof SPPs decreases as the frequency increases, as shown in Figure 4c. In particular, a cut-off frequency at ~1.2 THz is observed, indicating that the spoof SPPs above such a frequency cannot be guided anymore [44]. By varying the depth d and the duty cycle w/p of the grooves, the propagation characteristics of the waveguide can be tailored [45]. When the geometry of the grooves is adjusted to the wavelength-scale, the cut-off frequency will accordingly shift to a lower frequency range, in turn narrowing the operating bandwidth. However, it is impossible to introduce any bandgaps into the operating bandwidth by solely engraving grooves with a single periodicity.

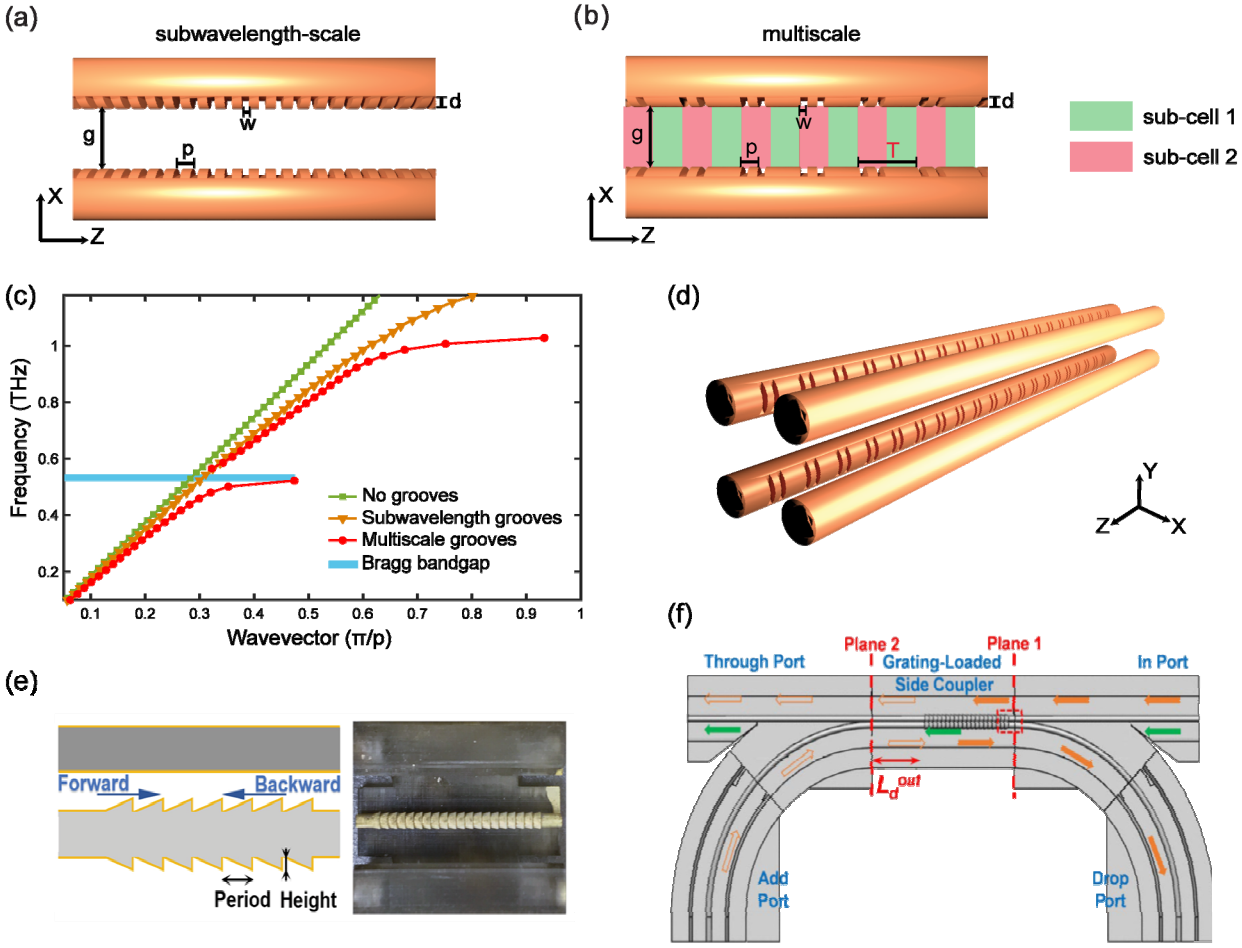

Figure 4. THz metal−wire signal processors realized by engineering the wire surfaces. (**a**) Schematic of the TWWG (a wire radius r = 127 μm, an air gap g = 300 μm) with subwavelength-scale periodic grooves, adapted from [41]. Geometry of the grooves: width w = 35 μm, depth d = 40 μm, and period p = 80 μm. (**b**) Schematic of the TWWG with multiscale grooves. This structure results from superimposing a wavelength-scale periodic modulation with a period of T = 280 μm onto the subwavelength-scale periodic grooves in (**a**), adapted from [41]. (**c**) Simulated dispersion relations of the plain TWWG (in green), and TWWGs with subwavelength-scale (in orange) and multiscale periodic grooves (in red), adapted from [41]. (**d**) Schematic of the FWWG with integrated multiscale-structured Bragg gratings, adapted from [41]. (**e**) Schematic of the Bragg grating achieved via 3D-printing, adapted from [39]. The grating contains 20 periods featuring a period Λ = 1.03 mm and a grating height H = 0.21 mm. (**f**) Schematic of the four-port add-drop multiplexer realized via 3D printing, adapted from [39]. It is composed of two Y splitters and a 35-mm-long grating-loaded side coupler.

To overcome these issues, Dong et al. introduced the concept of multiscale structures into the THz regime [41]. As shown in Figure 4b, a multiscale structure can be realized by superimposing a wavelength-scale periodic modulation onto the subwavelength-scale periodic grooves. The corresponding dispersion relation confirms the occurrence of a Bragg bandgap while maintaining the overall bandwidth. The location of the Bragg bandgap can be easily tuned over the operating bandwidth by varying the wavelength-scale modulation T. The concept of engraving grooves with multiscale structures, which combines the merits of photonic crystal and metamaterials, can offer additional degrees of freedom to tailor the spectral response of the entire structure. Based on this concept, a TWWG with an integrated Bragg grating was fabricated, featuring a Bragg resonance at ~0.53 THz with a notch depth of ~25 dB [41]. The fabrication of periodic grooves on bare copper wires can be

realized by using an automatic dicing saw. The thickness of the employed diamond blade determines the width of the grooves, where the grooves along the wires can be realized by utilizing a 3D motorized control of the dicing saw. Furthermore, by integrating the multiscale-structured Bragg grating into the FWWG, as shown in Figure 4d, Dong et al. demonstrated a broadband polarization-division multiplexer, in which a notch filtering is enabled for one target (x-polarized) channel without influencing the all-pass filtering of the other (y-polarized) channel, in turn leading to the realization of independent manipulation of THz multiplexed signals [41].

Besides engraving grooves on the wires using a diamond blade, another promising method to engineer the wire surfaces is to first print the wires with designed structures and then metallize the exposed surfaces. In [39], a TWWG integrated Bragg grating was fabricated by printing a sequence of end-to-end connected truncated cones added on top of a uniform wire, as shown in Figure 4e. The choice of truncated cones in the grating structure was experimentally found to be the most reliable and stable for 3D printing. Such Bragg gratings typically feature high grating strength and wide stopbands, given their strong geometrical overlap with the modal field confined in the gap between two wires. The experimental characterization of a 20-period Bragg grating demonstrated a pronounced transmission dip around 0.14 THz with a bandwidth of ~18 GHz [39]. Furthermore, by combining the waveguide integrated Bragg grating with the Y-shaped coupler and the side coupler (introduced in the previous sections), all fabricated using 3D printing and surface metallization techniques, a four-port THz add-drop multiplexer was realized [39]. Such a device allows for dropping the THz channels with frequencies that fall within the stopband of the Bragg grating, while letting all the other channels within the bandwidth of the side coupler to pass through. This approach provides a robust integrated solution for frequency-domain multiplexing and demultiplexing of THz signals.

It is worth noting that the majority of the metal-wire signal processors discussed in this review rely on the realization of waveguide-integrated Bragg gratings. Therefore, the evaluation of the device performance involves the calculation of the quality factor, i.e., the Q-factor, of the Bragg resonances. Such quantity is defined as the ratio between the resonance frequency f_c and the 3 dB-stopband Δf symmetrically measured across f_c, $Q = f_c/\Delta f$. In Table 2, the Q-factors of various waveguide-integrated Bragg gratings fabricated using different techniques are listed.

Table 2. The Q-factors of waveguide-integrated Bragg gratings fabricated using different techniques.

Reference	Method	f_c	Q-Factor
Yan et al. [38]	Laser cutting on papers	0.637 THz	142
Cao et al. [37]	Hot stamping + metal deposition	0.14 THz	4.4
Cao et al. [39]	3D printing + metal deposition	0.14 THz	7.8
Dong et al. [41]	Directly engraving wire surfaces	0.53 THz	479.5

4. Perspectives

In conclusion, we have summarized the three current methodologies for the realization of broadband THz metal-wire signal processors, including inserting standalone components, varying waveguide topologies and geometries, as well as engineering wire surfaces. By the joint applications of these methodologies, more complex functionalities can be achieved. Future research will focus on enabling THz metal-wire signal processors with tunability. This can be obtained by inserting 2D artificial material sheets, such as graphene [46] and transition metals dichalcogenides [47], that can be tuned electrically or optically. In addition, novel metasurface-based devices [48] that feature ultrafast optical/electrical modulation properties can also be introduced into the metal-wire waveguides. Moreover, emerging concepts, such as topological insulators [49], can be incorporated into the design of wire surfaces, which shows great potential towards the realization of unprecedented signal-processing functionalities. Finally, driven by the recent advances in machine learning techniques [50], the possibilities of developing machine-learning-enabled THz

signal processors is attracting increasing interest. By exploiting additive manufacturing techniques, the design generated by machine learning algorithms can be easily realized, in turn leading to the fabrication of robust, cost-effective, and highly reconfigurable THz signal processors. We envision that, with the current, rapid evolution of THz technology, metal-wire signal processors will achieve ubiquitous applications which combine extreme data-rates with agility, reliability, zero response time, and artificial intelligence, such as the transmission of uncompressed ultra-high-definition video, holographic communications, as well as chip-to-chip communications.

Author Contributions: Conceptualization, J.D. and R.M.; writing—original draft preparation, M.G. and J.D.; writing—review and editing, J.D. and R.M.; visualization, A.A.; supervision, J.D. and R.M.; project administration, R.M.; funding acquisition, R.M. All authors have read and agreed to the published version of the manuscript.

Funding: This research was funded by the Natural Sciences and Engineering Research Council of Canada (NSERC) through the Discovery, Strategic, and the Canada Research Chair programs.

Institutional Review Board Statement: Not applicable.

Informed Consent Statement: Not applicable.

Data Availability Statement: Not applicable.

Conflicts of Interest: The authors declare no conflict of interest.

References

1. Dang, S.; Amin, O.; Shihada, B.; Alouini, M. What Should 6G Be ? *Nat. Electron.* **2020**, *3*, 20–29. [CrossRef]
2. Calvanese Strinati, E.; Barbarossa, S.; Gonzalez-Jimenez, J.L.; Ktenas, D.; Cassiau, N.; Maret, L.; Dehos, C. 6G: The Next Frontier: From Holographic Messaging to Artificial Intelligence Using Subterahertz and Visible Light Communication. *IEEE Veh. Technol. Mag.* **2019**, *14*, 42–50. [CrossRef]
3. Saad, W.; Bennis, M.; Chen, M. A Vision of 6G Wireless Systems: Applications, Trends, Technologies, and Open Research Problems. *IEEE Netw.* **2020**, *34*, 134–142. [CrossRef]
4. Rappaport, T.S.; Xing, Y.; Kanhere, O.; Ju, S.; Madanayake, A.; Mandal, S.; Alkhateeb, A.; Trichopoulos, G.C. Wireless Communications and Applications Above 100 GHz: Opportunities and Challenges for 6G and Beyond. *IEEE Access* **2019**, *7*, 78729–78757. [CrossRef]
5. Nagatsuma, T.; Ducournau, G.; Renaud, C.C. Advances in Terahertz Communications Accelerated by Photonics. *Nat. Photonics* **2016**, *10*, 371–379. [CrossRef]
6. Atakaramians, S.; Afshar, V.S.; Monro, T.M.; Abbott, D. Terahertz Dielectric Waveguides. *Adv. Opt. Photonics* **2013**, *5*, 169. [CrossRef]
7. Weidenbach, M.; Jahn, D.; Rehn, A.; Busch, S.F.; Beltrán-Mejía, F.; Balzer, J.C.; Koch, M. 3D Printed Dielectric Rectangular Waveguides, Splitters and Couplers for 120 GHz. *Opt. Express* **2016**, *24*, 28968. [CrossRef]
8. Cruz, A.; Cordeiro, C.; Franco, M. 3D Printed Hollow-Core Terahertz Fibers. *Fibers* **2018**, *6*, 43. [CrossRef]
9. Khan, M.T.A.; Li, H.; Duong, N.N.M.; Blanco-Redondo, A.; Atakaramians, S. 3D-Printed Terahertz Topological Waveguides. *Adv. Mater. Technol.* **2021**, *6*, 2100252. [CrossRef]
10. Nallappan, K.; Cao, Y.; Xu, G.; Guerboukha, H.; Nerguizian, C.; Skorobogatiy, M. Dispersion-Limited versus Power-Limited Terahertz Communication Links Using Solid Core Subwavelength Dielectric Fibers. *Photonics Res.* **2020**, *8*, 1757. [CrossRef]
11. Ma, T.; Nallapan, K.; Guerboukha, H.; Skorobogatiy, M. Analog Signal Processing in the Terahertz Communication Links Using Waveguide Bragg Gratings: Example of Dispersion Compensation. *Opt. Express* **2017**, *25*, 11009. [CrossRef]
12. Atakaramians, S.; Afshar, V.S.; Ebendorff-Heidepriem, H.; Nagel, M.; Fischer, B.M.; Abbott, D.; Monro, T.M. THz Porous Fibers: Design, Fabrication and Experimental Characterization. *Opt. Express* **2009**, *17*, 14053. [CrossRef]
13. Ung, B.; Mazhorova, A.; Dupuis, A.; Rozé, M.; Skorobogatiy, M. Polymer Microstructured Optical Fibers for Terahertz Wave Guiding. *Opt. Express* **2011**, *19*, B848. [CrossRef]
14. Bao, H.; Nielsen, K.; Rasmussen, H.K.; Jepsen, P.U.; Bang, O. Fabrication and Characterization of Porous-Core Honeycomb Bandgap THz Fibers. *Opt. Express* **2012**, *20*, 29507. [CrossRef]
15. Faisal, M.; Shariful Islam, M. Extremely High Birefringent Terahertz Fiber Using a Suspended Elliptic Core with Slotted Airholes. *Appl. Opt.* **2018**, *57*, 3340. [CrossRef]
16. Islam, M.S.; Cordeiro, C.M.B.; Franco, M.A.R.; Sultana, J.; Cruz, A.L.S.; Abbott, D. Terahertz Optical Fibers [Invited]. *Opt. Express* **2020**, *28*, 16089. [CrossRef]
17. Gallot, G.; Jamison, S.P.; McGowan, R.W.; Grischkowsky, D. Terahertz Waveguides. *J. Opt. Soc. Am. B* **2000**, *17*, 851. [CrossRef]
18. Navarro-Cía, M.; Wu, J.; Liu, H.; Mitrofanov, O. Generation of Radially-Polarized Terahertz Pulses for Coupling into Coaxial Waveguides. *Sci. Rep.* **2016**, *6*, 38926. [CrossRef]

19. Mendis, R.; Grischkowsky, D. Undistorted Guided-Wave Propagation of Subpicosecond Terahertz Pulses. *Opt. Lett.* **2001**, *26*, 846. [CrossRef]
20. Pahlevaninezhad, H.; Darcie, T.E.; Heshmat, B. Two-Wire Waveguide for Terahertz. *Opt. Express* **2010**, *18*, 7415. [CrossRef]
21. Markov, A.; Guerboukha, H.; Skorobogatiy, M. Hybrid Metal Wire–Dielectric Terahertz Waveguides: Challenges and Opportunities [Invited]. *J. Opt. Soc. Am. B* **2014**, *31*, 2587. [CrossRef]
22. Li, H.; Atakaramians, S.; Lwin, R.; Tang, X.; Yu, Z.; Argyros, A.; Kuhlmey, B.T. Flexible Single-Mode Hollow-Core Terahertz Fiber with Metamaterial Cladding. *Optica* **2016**, *3*, 941. [CrossRef]
23. Sengupta, K.; Nagatsuma, T.; Mittleman, D.M. Terahertz Integrated Electronic and Hybrid Electronic–Photonic Systems. *Nat. Electron.* **2018**, *1*, 622–635. [CrossRef]
24. Reichel, K.S.; Mendis, R.; Mittleman, D.M. A Broadband Terahertz Waveguide T-Junction Variable Power Splitter. *Sci. Rep.* **2016**, *6*, 28925. [CrossRef] [PubMed]
25. Reichel, K.S.; Lozada-Smith, N.; Joshipura, I.D.; Ma, J.; Shrestha, R.; Mendis, R.; Dickey, M.D.; Mittleman, D.M. Electrically Reconfigurable Terahertz Signal Processing Devices Using Liquid Metal Components. *Nat. Commun.* **2018**, *9*, 4202. [CrossRef]
26. Karl, N.J.; McKinney, R.W.; Monnai, Y.; Mendis, R.; Mittleman, D.M. Frequency-Division Multiplexing in the Terahertz Range Using a Leaky-Wave Antenna. *Nat. Photonics* **2015**, *9*, 717–720. [CrossRef]
27. Mbonye, M.; Mendis, R.; Mittleman, D.M. A Terahertz Two-Wire Waveguide with Low Bending Loss. *Appl. Phys. Lett.* **2009**, *95*, 1–4. [CrossRef]
28. Shrestha, R.; Kerpez, K.; Hwang, C.S.; Mohseni, M.; Cioffi, J.M.; Mittleman, D.M. A Wire Waveguide Channel for Terabit-per-Second Links. *Appl. Phys. Lett.* **2020**, *116*, 131102. [CrossRef]
29. Wang, K.; Mittleman, D.M. Metal Wires for Terahertz Wave Guiding. *Nature* **2004**, *432*, 376–379. [CrossRef]
30. Maier, S.A.; Andrews, S.R.; Martín-Moreno, L.; García-Vidal, F.J. Terahertz Surface Plasmon-Polariton Propagation and Focusing on Periodically Corrugated Metal Wires. *Phys. Rev. Lett.* **2006**, *97*, 176805. [CrossRef]
31. Astley, V.; Scheiman, J.; Mendis, R.; Mittleman, D.M. Bending and Coupling Losses in Terahertz Wire Waveguides. *Opt. Lett.* **2010**, *35*, 553. [CrossRef] [PubMed]
32. Wang, K.; Mittleman, D.M. Dispersion of Surface Plasmon Polaritons on Metal Wires in the Terahertz Frequency Range. *Phys. Rev. Lett.* **2006**, *96*, 157401. [CrossRef] [PubMed]
33. Cao, H.; Nahata, A. Coupling of Terahertz Pulses onto a Single Metal Wire Waveguide Using Milled Grooves. *Opt. Express* **2005**, *13*, 7028. [CrossRef]
34. Mridha, M.K.; Mazhorova, A.; Clerici, M.; Al-Naib, I.; Daneau, M.; Ropagnol, X.; Peccianti, M.; Reimer, C.; Ferrera, M.; Razzari, L.; et al. Active Terahertz Two-Wire Waveguides. *Opt. Express* **2014**, *22*, 22340. [CrossRef] [PubMed]
35. Lee, Y.-S. *Principles of Terahertz Science and Technology*; Springer: Boston, MA, USA, 2009; ISBN 978-0-387-09539-4.
36. Markov, A.; Skorobogatiy, M. Two-Wire Terahertz Fibers with Porous Dielectric Support. *Opt. Express* **2013**, *21*, 12728. [CrossRef] [PubMed]
37. Cao, Y.; Nallappan, K.; Guerboukha, H.; Xu, G.; Skorobogatiy, M. Additive Manufacturing of Highly Reconfigurable Plasmonic Circuits for Terahertz Communications. *Optica* **2020**, *7*, 1112. [CrossRef]
38. Yan, G.; Markov, A.; Chinifooroshan, Y.; Tripathi, S.M.; Bock, W.J.; Skorobogatiy, M. Low-Loss Terahertz Waveguide Bragg Grating Using a Two-Wire Waveguide and a Paper Grating. *Opt. Lett.* **2013**, *38*, 3089. [CrossRef]
39. Cao, Y.; Nallappan, K.; Xu, G.; Skorobogatiy, M. Add Drop Multiplexers for Terahertz Communications Using Two-Wire Waveguide-Based Plasmonic Circuits. *Nat. Commun.* **2022**, *13*, 4090. [CrossRef]
40. Balistreri, G.; Tomasino, A.; Dong, J.; Yurtsever, A.; Stivala, S.; Azaña, J.; Morandotti, R. Time-Domain Integration of Broadband Terahertz Pulses in a Tapered Two-Wire Waveguide. *Laser Photon. Rev.* **2021**, *15*, 2100051. [CrossRef]
41. Dong, J.; Tomasino, A.; Balistreri, G.; You, P.; Vorobiov, A.; Charette, É.; Le Drogoff, B.; Chaker, M.; Yurtsever, A.; Stivala, S.; et al. Versatile Metal-Wire Waveguides for Broadband Terahertz Signal Processing and Multiplexing. *Nat. Commun.* **2022**, *13*, 741. [CrossRef]
42. Shen, L.; Chen, X.; Zhong, Y.; Agarwal, K. Effect of Absorption on Terahertz Surface Plasmon Polaritons Propagating along Periodically Corrugated Metal Wires. *Phys. Rev. B* **2008**, *77*, 075408. [CrossRef]
43. Meng, Y.; Xiang, H.; Zhang, R.-Y.; Wu, X.; Han, D.; Chan, C.T.; Wen, W. Topological Interface States in Multiscale Spoof-Insulator-Spoof Waveguides. *Opt. Lett.* **2016**, *41*, 3698. [CrossRef]
44. Fu, Z.; Gan, Q.; Ding, Y.J.; Bartoli, F.J. From Waveguiding to Spatial Localization of THz Waves within a Plasmonic Metallic Grating. *IEEE J. Sel. Top. Quantum Electron.* **2008**, *14*, 486–490. [CrossRef]
45. Gan, Q.; Fu, Z.; Ding, Y.J.; Bartoli, F.J. Ultrawide-Bandwidth Slow-Light System Based on THz Plasmonic Graded Metallic Grating Structures. *Phys. Rev. Lett.* **2008**, *100*, 256803. [CrossRef] [PubMed]
46. Xia, S.-X.; Zhai, X.; Wang, L.-L.; Wen, S.-C. Plasmonically Induced Transparency in Double-Layered Graphene Nanoribbons. *Photonics Res.* **2018**, *6*, 692. [CrossRef]
47. Gopalan, P.; Sensale-Rodriguez, B. 2D Materials for Terahertz Modulation. *Adv. Opt. Mater.* **2020**, *8*, 1900550. [CrossRef]
48. He, W.; Tong, M.; Xu, Z.; Hu, Y.; Cheng, X.; Jiang, T. Ultrafast All-Optical Terahertz Modulation Based on an Inverse-Designed Metasurface. *Photonics Res.* **2021**, *9*, 1099. [CrossRef]

49. Zangeneh-Nejad, F.; Fleury, R. Topological Analog Signal Processing. *Nat. Commun.* **2019**, *10*, 2058. [CrossRef]
50. Mengu, D.; Sakib Rahman, M.S.; Luo, Y.; Li, J.; Kulce, O.; Ozcan, A. At the Intersection of Optics and Deep Learning: Statistical Inference, Computing, and Inverse Design. *Adv. Opt. Photonics* **2022**, *14*, 209. [CrossRef]